Research Article | Vol. 24, No. 22 | 31 Oct 2016 | OPTICS EXPRESS 24846

Optics EXPRESS

Freeform microlens array homogenizer for excimer laser beam shaping

YUHUA JIN,* ALI HASSAN, AND YIJIAN JIANG

Institute of Laser Engineering, Beijing University of Technology, Beijing 100124, China
**ultra_jin@outlook.com*

Abstract: We presented a novel technique to design microlens optical beam homogenizing system for excimer lasers. As a new approach by applying freeform surface microlens array, the homogenizer can yield somehow superior beam shaping results with larger but less microlens units than conventional method. With new concept and design, the diffraction effects at the microlens apertures can be reduced substantially. Large scale and highly uniform beam profile can be realized at a relative nearby working distance after beam shaping. This is hard to achieve by conventional method. Our design method takes the real spatial energy characteristics of the excimer laser beam as the design basis, and combined with feasible optimization method. The design method is demonstrated as a real instance based, on a 193 nm ArF excimer laser in our laboratory. Moreover, to verify the effectiveness of our method, the designed freeform microlens array homogenizer has been fabricated and tested experimentally. The experimental optical performance of the homogenizer coincides well with the theoretical simulation.

OCIS codes: (140.3300) Laser beam shaping; (080.4298) Nonimaging optics; (220.2945) Illumination design; (080.4225) Nonspherical lens design; (140.3610) Lasers, ultraviolet.

References and links

1. J. J. Ewing, "Excimer lasers at 30 years," Opt. Photonics News **14**(5), 26–31 (2003).
2. R. Delmdahl and R. Pätzel, "Excimer laser technology trends," J. Phys. D Appl. Phys. **47**(3), 034004 (2014).
3. G. Jin, S. Choi, M. Kim, S. Kim, and J. Song, "New pixel circuit design employing an additional pixel line insertion in AMOLED displays composed by excimer laser-crystallized TFTs," J. Disp. Technol. **8**(8), 479–482 (2012).
4. S. Beke, B. Farkas, I. Romano, and F. Brandi, "3D scaffold fabrication by mask projection excimer laser stereolithography," Opt. Mater. Express **4**(10), 2032–2041 (2014).
5. H. Fukuda, Y. Yoo, Y. Minegishi, N. Hisanaga, and T. Enami, "Advanced excimer laser technologies enable green semiconductor manufacturing," Proc. SPIE **9052**, 90522J (2014).
6. Y. Liu and Y. Jiang, "Rapid fabrication of patterned high-performance conductor poly (vinylidene fluoride) surfaces using a 248nm excimer laser," Opt. Express **18**(21), 22041–22046 (2010).
7. R. Beal, V. Aimez, and J. J. Dubowski, "Excimer laser induced quantum well intermixing: a reproducibility study of the process for fabrication of photonic integrated devices," Opt. Express **23**(2), 1073–1080 (2015).
8. C. Dorronsoro, L. Remon, J. Merayo-Lloves, and S. Marcos, "Experimental evaluation of optimized ablation patterns for laser refractive surgery," Opt. Express **17**(17), 15292–15307 (2009).
9. S. Beggs, J. Short, M. Rengifo-Pardo, and A. Ehrlich, "Applications of the excimer laser: a review," Dermatol. Surg. **41**(11), 1201–1211 (2015).
10. M. E. Johnson and E. Voigtman, "Temporal and spectral characteristics of the output of an excimer laser," Appl. Spectrosc. **44**(6), 958–961 (1990).
11. A. Masters and T. Geuking, "Beam shaping optics expand excimer-laser applications," Laser Focus World **41**(6), 99–101 (2005).
12. F. M. Dickey, T. E. Lizotte, S. C. Holswade, and D. L. Shealy, *Laser Beam Shaping Applications*, 1st ed. (CRC Press, 2005).
13. R. F. Pease and S. Y. Chou, "Lithography and other patterning techniques for future electronics," Proc. IEEE **96**(2), 248–270 (2008).
14. F. M. Dickey, *Laser Beam Shaping: Theory and Techniques*, 2nd ed. (CRC Press, 2014).
15. K. Jasper, S. Scheede, B. Burghardt, R. Senczuk, P. Berger, H. J. Kahlert, and H. Hugel, "Excimer laser beam homogenizer with low divergence," Appl. Phys., A Mater. Sci. Process. **69**(7), S315–S318 (1999).
16. J. Turunen, P. Paallonen, M. Kuittinen, P. Laakkonen, J. Simonen, T. Kajava, and M. Kaivola, "Diffractive shaping of excimer laser beams," J. Mod. Opt. **47**(13), 2467–2475 (2000).
17. M. Burkhardt and R. Brunner, "Functional integrated optical elements for beam shaping with coherence scrambling property, realized by interference lithography," Appl. Opt. **46**(28), 7061–7067 (2007).

#274644 http://dx.doi.org/10.1364/OE.24.024846
Journal © 2016 Received 31 Aug 2016; revised 7 Oct 2016; accepted 13 Oct 2016; published 17 Oct 2016

Optics EXPRESS

18. Y. Matsuura, D. Akiyama, and M. Miyagi, "Beam homogenizer for hollow-fiber delivery system of excimer laser light," Appl. Opt. **42**(18), 3505–3508 (2003).
19. M. Zimmermann, N. R. V. Lindlein, and K. J. Weible, "Microlens laser beam homogenizer—from theory to application," Proc. SPIE **6663**, 666302 (2007).
20. Y. Lin, G. N. Lawrence, and J. Buck, "Characterization of excimer lasers for application to lenslet array homogenizers," Appl. Opt. **40**(12), 1931–1941 (2001).
21. A. Buttner and U. D. Zeitner, "Wave optical analysis of light-emitting diode beam shaping using microlens arrays," Opt. Eng. **41**(10), 2393–2401 (2002).
22. P. J. Smilie and T. J. Suleski, "Variable-diameter refractive beam shaping with freeform optical surfaces," Opt. Lett. **36**(21), 4170–4172 (2011).
23. Z. Feng, L. Huang, M. Gong, and G. Jin, "Beam shaping system design using double freeform optical surfaces," Opt. Express **21**(12), 14728–14735 (2013).
24. Z. Feng, L. Huang, G. Jin, and M. Gong, "Designing double freeform optical surfaces for controlling both irradiance and wavefront," Opt. Express **21**(23), 28693–28701 (2013).
25. R. Wu, P. Liu, Y. Zhang, Z. Zheng, H. Li, and X. Liu, "A mathematical model of the single freeform surface design for collimated beam shaping," Opt. Express **21**(18), 20974–20989 (2013).
26. Z. Feng, B. D. Froese, and R. Liang, "Composite method for precise freeform optical beam shaping," Appl. Opt. **54**(31), 9364–9369 (2015).
27. Y. Jin, Y. Zhao, and Y. Jiang, "Microlens beam homogenizer for excimer laser processing," J. Laser Appl. **28**(2), 022601 (2016).
28. D. Salomon, *Curves and Surfaces for Computer Graphics* (Springer, 2005).
29. I. Kaya, "Mathematical and computational methods for freeform optical shape description," Diss. Department of Electrical Engineering and Computer Science, University of Central Florida (2013).
30. K. Fuerschbach, J. P. Rolland, and K. P. Thompson, "A new family of optical systems employing φ-polynomial surfaces," Opt. Express **19**(22), 21919–21928 (2011).
31. K. Rahbar, K. Faez, and E. Attaran Kakhki, "Phase wavefront aberration modeling using Zernike and pseudo-Zernike polynomials," J. Opt. Soc. Am. A **30**(10), 1988–1993 (2013).
32. K. Fuerschbach, K. P. Thompson, and J. P. Rolland, "Interferometric measurement of a concave, φ-polynomial, Zernike mirror," Opt. Lett. **39**(1), 18–21 (2014).
33. J. C. Mason and D. C. Handscomb, *Chebyshev Polynomials*, 1st ed. (Chapman and Hall/CRC, 2002).
34. S. Kudaev and P. Schreiber, "Automated optimization of nonimaging optics for luminaires," Proc. SPIE **5962**, 59620B (2005).

1. Introduction

Excimer lasers are powerful and versatile Lasing sources in the UV range of the electromagnetic spectra. Because of their high pulse energies, high average power, cold ablation and shorter wavelength [1, 2], excimer lasers have countless applications, not only in the field of industrial manufacturing [3–5], but also in the field of scientific research [6, 7] and medical treatment [8, 9].

Typically, because of the beam generation mechanism, the pattern of excimer laser beam profile is rendered as an approximate rectangular or even more irregular shape, also accompanied with complex spatial energy distribution [10]. To overcome this drawback, the raw beam produced by most excimer lasers must be reshaped or homogenized to match the applications needs [11]. Actually, the vast majority of those applications which image a mask pattern onto the work plane, requires a uniform distribution of radiation intensity over the whole mask area, then consequently obtain high quality and uniform beam pattern on the targeted work plane [12]. The most representative examples are the DUV optical lithography technique for semiconductor manufacturing [13] and the production of nozzle plates for inkjet printers [14].

However, as most excimer lasers do not export laser pulses with well-behaved, regular Gaussian profile, the beam shaping transformation cannot be realized just by commercial optical systems used for common lasers. For this challenge, various optical components and systems have been developed [15–18]. Among those approaches, the well-known type is the microlens array homogenizer [14], also known as the fly's eye homogenizer, because of its easy use and good homogenizing results.

The microlens array homogenizer belongs to multi-aperture beam integration systems. Purely in the case of geometrical optics, an increase of the number of microlenses across the pupil diameter will improve the quality and uniformity of the homogenized beam profile.

Optics EXPRESS

However, from the perspective of physical optics, the more microlenses used to split the beam means that smaller aperture of the microlens unit in the array should be, and that will bring an undesirable increase of diffraction effects, which can affect the homogenization result significantly [19]. Meanwhile, if the illumination distance is specified, simply reducing the aperture of microlens unit to improve the beam uniformity will also reduce the illumination area. When a mask is illuminated by a beam homogenizer, then unmagnified and imaged onto a work piece, the larger illumination field means the more details of the mask can be projected and more precise microstructures can be ablated [14]. Besides these, in terms of general thinking to achieve an excellent beam uniformity for excimer laser, the amount of microlenses may be up to many thousands and the microlens unit will be decreased to micron scale [11, 19], and the miniaturization of the microlenses poses a potentially serious challenge to the assembly of the optical components [20].

In this paper, we presented a novel method to design microlens beam homogenizing optical system for excimer laser. As a new approach we applied a freeform microlens array surface as the first optical component of the homogenizer. Each effective freeform surface in the array introduces appropriate aberrations in the wavefront to redistribute the irradiance of the beam. With larger but less microlens units, the homogenizer can yield somehow superior beam shaping results than conventional microlens array homogenizer. Our design method takes account of the real spatial energy characteristics of the excimer laser beam, thus provides better stability and practicality than ordinary designs. The applicative advantages of the new concept and design are also presented and discussed.

For simple understanding, the design method is demonstrated as a real instance based, on a 193 nm ArF excimer laser in our laboratory. In Sec. 2, some key issues of the basic optical design of the microlens array homogenizer have been discussed. Combining with simulation, the specific design method is presented in Sec. 3. To verify design method, the designed freeform microlens array homogenizer has been fabricated and experimentally verified. Measurements of the beam shaping results are presented in Sec. 4.

2. Design considerations of microlens array homogenizer

The basic optical design principles of microlens array homogenizer have been discussed in [14] and [19]. The main content discussed in this section addresses the situation for excimer laser.

2.1 Basic design considerations

All multi-aperture microlens array beam homogenizer can be loosely divided into two categories: non-imaging and imaging. The fundamental difference between the two types of homogenizers is that the non-imaging version uses a single lens array and a spherical Fourier lens, whereas the imaging version uses two lens arrays and a spherical Fourier lens. Both types have the same optical mechanism that they utilize sub aperture microlens array to segment the entrance pupil or cross section of the incident beam into an array of beamlets. When these beamlets passes through the spherical Fourier lens, they converged and overlapped at the same position on the target illumination plane. In general, the imaging homogenizer composed of double microlens arrays can provide much better flat-top uniformity. Because of the intervention of the second microlens array, each microlens in the second array, in combination with spherical Fourier lens, can bring a field lens effect. Such a field lens array can provide overlapping images at the illumination plane for different fields from the source, thus both axial and diverging rays can be refracted to the target area of illumination [21]. As excimer laser beams always have complex spatial characteristics, it is a good choice to use the imaging framework as the design infrastructure. Here is worth noting that, general imaging homogenizers always employ two identical microlens arrays separated from each other by the focal length, but this is not a feasible solution for excimer lasers. Because the excimer laser beam has a high average power in the UV to DUV range, it can be

Optics EXPRESS

easily absorbed by materials. Simply using two identical microlens arrays configuration will make the second microlens array ablated by the focusing energy of the first microlens array. In this case, the homogenizer should be composed by different microlens arrays. The preliminary structure of the homogenizer is illustrated in Fig. 1.

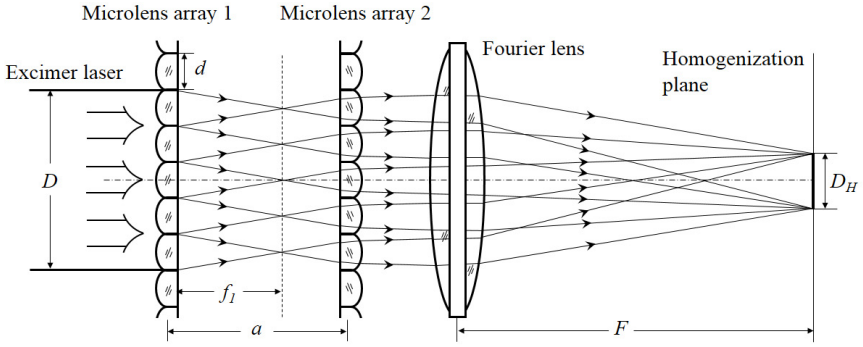

Fig. 1. Optical schematic illustration of optical microlens array homogenizer for excimer laser.

The fundamental design parameters which describe the homogenizer are: the diameter of input excimer laser beam D, the diameter of the microlens unit d, the diameter of the homogenized beam profile D_H, the focal length of the first microlens array f_1, the focal length of the second microlens array f_2 (not shown in Fig. 1), and the focal length of the Fourier lens F.

In order to form beam channels to let beamlets passes through smoothly, both microlens arrays have a same microlens unit diameter d. And to ensure a high optical fill factor, both arrays employ square aperture units, thus helps to generate a square beam profile according to the imaging theory. In addition, as shown in Fig. 1, the optical surfaces of two microlens arrays possess inverse orientations. Actually, the optical surface orientation of microlens array does not significantly affect beam homogenizing. However, for imaging optics perspective, the same optical surface orientations do not contribute to the offsetting of spherical aberration. The spherical aberrations belonging to the sub apertures can be presented at the target illumination plane, and consequently cause a distortion in the beam profile finally.

Assuming that all components of the homogenizer are in ideal optics, the paraxial approximation and standard thin lens equations can be used to drive the correlation between the design parameters. The dimensions of the homogenized beam profile is given by

$$D_H = d\frac{F}{f_1 \cdot f_2}\left[\left(f_1 + f_2\right) - a\right]. \tag{1}$$

Note that homogenized plane size is now dependent not only on the focal lengths of all three components, but also on the separation of two microlens arrays. According to the general imaging conditions, it can be considered that the separation between two microlens arrays equals to the focal length of the second microlens array, i.e. $a \approx f_2$. With this approximate relationship, Eq. (1) can be simplified as

$$D_H = d\frac{F}{a}. \tag{2}$$

If the effective working distance of the homogenizer has been determined, in other words, the value of F has been specified, the dimension of the homogenized beam profile D_H is only proportional to d and inversely proportional to a. That means if a larger illumination field is needed in design, there are only two ways to achieve the performance: to increase the

Optics EXPRESS

diameter of microlens unit cell or to decrease the separation between two microlens arrays. However, as we mentioned in Sec. 1, simply enlarging the sub apertures of the microlens arrays will adversely affect homogenization result. Whereas reducing the space between two microlens arrays is not practicable enough, because the second microlens array should always be kept away from the focal plane of the first microlens array. Although shortening in the focal length of the first microlens array could maintain the constraint, but the solution does not work very effectively. Moreover, for spherical microlens units, the shorter focal length means the larger curvature of the optical surface, hence pronounces much more spherical aberration which can also distort the shape of the homogenized beam profile.

2.2 Diffraction considerations

Over many years of exploration and development on beam shaping techniques, the standards of irradiation uniformity for different laser applications have been formed objectively. Broadly, the standards can be divided into three progressive levels: ordinary beam uniformity within ± 5% (e.g. for general laser micromachining applications), good beam uniformity within ± 2% (e.g. for elementary optical lithography), and excellent beam uniformity within ± 1.5% (e.g. for sophisticated optical lithography, inkjet nozzle drilling or silicon crystallization) [11, 12, 14, 19]. In realistic applications, of course, the higher beam uniformity produces better processing quality. For commercial excimer lasers, the vertical and horizontal beam dimensions are always on centimeter scale, and to obtain a good beam uniformity by microlens array homogenizer, the microlens units could be on micron scale. On such a scale, the diffraction effect produced by microlens unit cannot be ignored.

The diffraction pattern of a single sub aperture determines the shape of beam profile on the target plane. This irradiance distribution can be quantified and estimated by the Fresnel number, which is an important quantity to characterize the influence of diffraction effects onto an optical lens. The Fresnel number (FN) equals the number of half-waves of optical path difference (OPD) and can be approximately given by

$$FN = 2 \times OPD = \frac{r^2}{\lambda}\left(\frac{1}{R_w} - \frac{1}{R_0}\right), \tag{3}$$

where r is the radial coordinate in the sub aperture, λ is the wavelength of the incident light beam, R_w is the radius of curvature of the wave front, and R_0 is the radius of curvature of a reference sphere centered on the observation point.

For convenience, assuming that a collimated laser beam (i.e. plane light wave) incident upon the microlens array with a fill factor of 100%, the optical powers of the microlens and the primary lens combine to produce a spherical wave front converging with a radius of curvature of R_w. If f is the focal length of the microlens unit and F is the focal length of the Fourier lens, substituting geometric relations $R_w^{-1} = f^{-1} + F^{-1}$, $R_0^{-1} = F^{-1}$, and $d = 2r$ into Eq. (3), the Fresnel number in terms of microlens parameters can be derived as

$$FN = \frac{d^2}{4\lambda \cdot f}. \tag{4}$$

Further, considering the general imaging conditions and substituting Eq. (2) into Eq. (4), the Fresnel number can be written in terms of the fundamental design parameters of the microlens homogenizer

$$FN = \frac{d \cdot D_H}{4\lambda \cdot F}. \tag{5}$$

In practice, the beam shaping result is related to Fresnel diffraction at the microlens array and the Fresnel diffraction is determined by the Fresnel number FN. The lower the Fresnel number, the more blurred the target pattern becomes. Conversely higher Fresnel number

Optics EXPRESS

produces sharper edge and smaller variation for the shaped beam profile. Equation (5) shows that if the effective working distance F of the homogenizer has been specified, the Fresnel number is only proportional to the diameter of the microlens unit cell d and the diameter of the shaped beam profile D_H. Since D_H is also proportional to "d" as discussed previously, the diameter of the microlens unit cell d should be the dominant factor to the Fresnel number. That means enlarging the sub aperture of the microlens array could not only create larger illumination field, but also gives sharper beam profile on the target plane. However, using microlens array with larger sub aperture is not conductive to improve the uniformity of the shaped beam profile. To solve this contradiction, we employ freeform microlenses to replace the regular units in the array. The details are presented in the next section.

3. New design method of freeform microlens array homogenizer

When the incident beam separated as sub beamlets by microlens array, each beamlet itself introduces a modulation for the flat-top intensity. In other words, the intensity distribution involved in each beamlet is directly related to the uniformity of homogenized beam profile. The microlens arrays with larger sub aperture and less unit cell amount cannot segment the incident beam meticulously enough, hence the beamlets cannot fill up or neutralize each other, and adequately the deficiency and excess of the energy distribution at the overlapped area occurs. Since freeform optics has been widely studied for light beam shaping [22–26], we come up with a solution that by employing freeform microlenses, one can compensate these drawbacks. Because of its high design degree of freedom, each freeform surface in the array can introduce appropriate aberrations in the wave front to redistribute the irradiance of the beamlet correspondingly, and so that to improve the uniformity of the overlapped beam profile.

Theoretically, the freeform optical design should be based on specified light sources and desired target illuminations, with establishing the mathematical relationship between the prescribed irradiance distributions and features of the optical surfaces to determine the spatial shapes of desired freeform surfaces. However for most excimer lasers, because the beam profiles can be distorted by their own conditions and operational environments, it is hard to accurately describe this kind of light source by purely mathematical equations. To improve this situation while enhancing the pertinence and effectiveness of the designed optical system, we collected the real intensity distribution for the excimer laser as a fundamental basis for optical design.

As a concrete instance, the excimer laser that was designed for test is a 193 nm ArF laser (LPXpro 305, Coherent, Inc.) in our laboratory, which delivers short intense pulses (up to 600 mJ/pulse, 25 ns pulse duration). The repetition rate of the pulses is up to 50Hz, continuously adjustable. The maximum average power can be stabilized at 20 W with the full repetition rate. We utilized a laser beam analyzer (LBA-USB-SP503U, Ophir Optronics, Inc.) to collect the spatial intensity distribution data of the initial excimer beam. The detector was placed in the optical axis, with a distance of 20 cm from the outlet window of the excimer laser where the initial beam will be incident upon the optical system. With the selection of trigger capture mode, the input signal from the CCD sensor is continuously monitored, and when a laser pulse is detected, the frame is captured. Besides, to avoid the negative effect to design caused by the fluctuation between the laser pulses, while give the design some tolerance to slight distortion or variation of the beam profile, pulses during a sufficiently long time were taken into account. The spatial intensity distribution data comes from a statistics set. With average processing, the initial excimer beam profile can be evaluated visually, as shown in Fig. 2.

The initial excimer beam profile is rendered as a rectangular pattern roughly, with significantly non-uniform intensity distribution. Notably, although we give the intensity distribution curves in the x and y directions, it is impossible to describe the beam profile thoroughly only by the two curves, because the intensity distribution of the profile is not axisymmetric completely, and that can be observed from Fig. 2(a) intuitively. Through

Optics EXPRESS

processing the collected spatial intensity distribution data, the excimer source can be simulated and represented in commercial optical design software, as shown in Fig. 3.

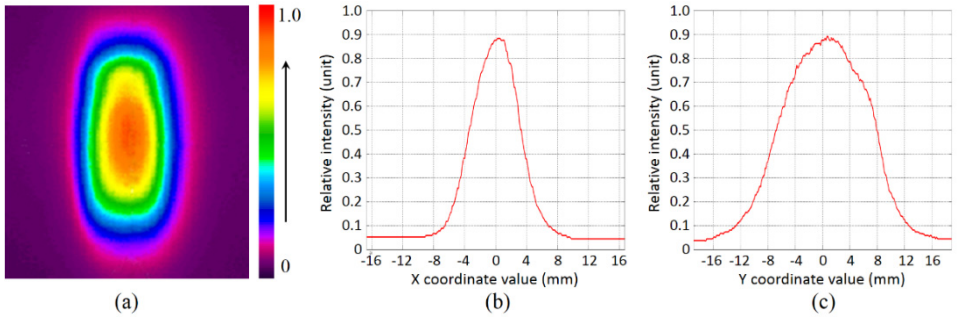

Fig. 2. Intensity distribution of the initial excimer beam profile. (a) Pseudo color image of the intensity distribution, (b) intensity distribution curve in the x direction, and (c) intensity distribution curve in the y direction.

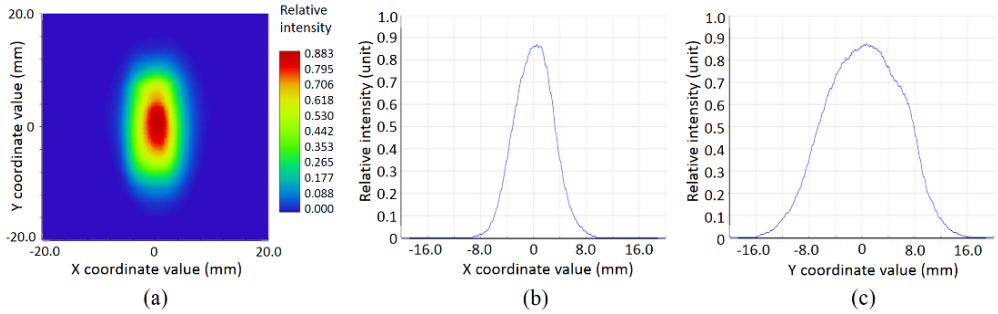

Fig. 3. Simulated incident excimer laser beam profile with Zemax Opticstudio. (a) Pseudo color image of intensity distribution on virtual detector, (b) normalized intensity distribution curve in the x direction, and (c) normalized intensity distribution curve in the y direction.

As the quantification of the spatial intensity distribution of the initial beam profile, the design work can be translated into an optimization of problem. The first step in the new design process is to utilize ordinary microlens arrays as the starting form to shape the excimer beam. This first step establishes the basic configuration parameters of the homogenizer, also determines the dimensions and the shape of the homogenized beam profile. Detailed process has been discussed in our previous work [27]. The next step is to replace spherical microlens surfaces with freeform surfaces, then optimize these freeform surfaces to introduce appropriate aberrations in the wave front to redistribute irradiance of each beamlet, so that to improve the uniformity of homogenized beam profile. However, from the experience of modern optical design, optimizing all the freeform microlenses at a time will involve too much variables, and that cannot make the iterative calculation converges effectively, thus resulting in dead ends. Roughly, there are 3 key factors to ensure the optimization be technically feasible, creating positive starting tendency for the optimization, selecting suitable objects to be optimized, and specifying reasonable variables as little as possible. To meet these factors, we present a part to whole optimization method, which is visually illustrated in Fig. 4.

After passing through the microlens array, each beamlet delivers its own partial irradiation energy of the initial laser beam, and that is imaged on the target plane. Obviously, each couple of axisymmetric beamlets have a tendency to create uniform irradiation when they overlap on the target irradiation plane, just as shown in Fig. 4(a). Based on this mechanism, each couple of axisymmetric microlenses in array 1 were specified as freeform optics to be

Optics EXPRESS

optimized respectively, as shown in Fig. 4(b). Theoretically, specifying microlenses in the array 2 as the freeform ones will also be able to introduce wavefront aberration to modify the irradiance in beamlet. However, because each beamlet intersection with the microlens units in array 2 does not have a full fill factor on the aperture, varying the sag of the surface can lead to a severe distortion for the edge of the shaped beam profile, which is hard to control during the actual optimization process.

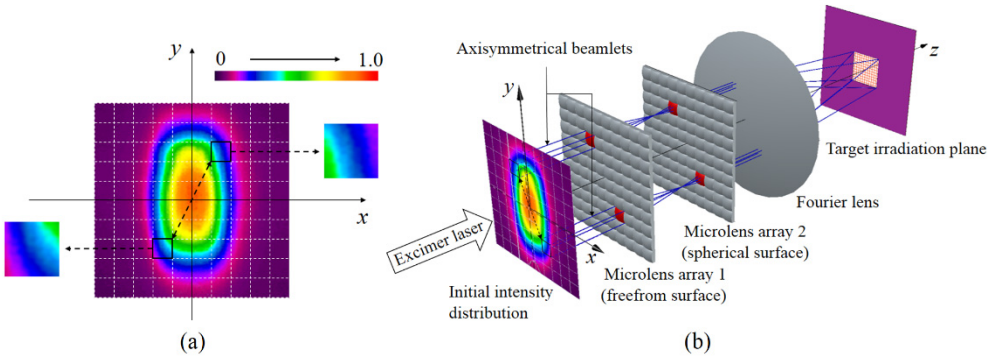

Fig. 4. Intuitive schematic of the optimization method. (a) A couple of axisymmetric beamlets. The energy intensity distributions have a complementary tendency to each other. (b) The visual relationship between optical elements. The microlenses in array 1 are specified as freeform ones.

Besides this, another point worth noting is the way to represent freeform surface. In most cases, freeform surfaces are characterized by the spatial control points of the designed surfaces, e.g. non-uniform rational B-spline (NURBS) surface and Bezier surface etc [28]. Nevertheless, considering a control point with three degrees of freedom (degrees of freedom manifest themselves as variables for optimization), which are x, y, and z positions in space. If each surface evaluation requires 10 × 10 points (a low estimate), simultaneously optimizing two surfaces would relate to 600 variables to calculate, and that is still a challenge for the optimization. Another way to describe freeform optical surface more easily is by the orthogonal polynomials [29]. The most representative one is the Zernike polynomials, which are widely used in optical design, wave front analysis, optical testing, etc [30–32]. However, the Zernike polynomial set is derived in polar coordinate system, thus it is not the best choice to contribute to a square illumination pattern. In the design, we quantify the freeform surfaces by the Chebyshev polynomials [33], which are based on Cartesian coordinate system. The Chebyshev polynomials of the first kind can be defined as the unique polynomials satisfying

$$T_n(x) = \cos(n \cdot \cos^{-1}(x)),\ n = 0...\infty,\ x \in [-1,1]. \tag{6}$$

Using a finite sum of the Chebyshev polynomial terms and applying the set into two-dimensional situation, the freeform surface can be described by the following equation

$$z = \frac{c(x^2 + y^2)}{1 + \sqrt{1 - c^2(x^2 + y^2)}} + \sum_{i=0}^{n}\sum_{j=0}^{m} c_{ij} T_i(\bar{x}) \cdot T_j(\bar{y}), \tag{7}$$

where z is the sag of the surface, c is the curvature for the base sphere on top of which the polynomial is added, x and y are the surface coordinates in the aperture, c_{ij} are the coefficients of the Chebyshev polynomial sum, $\bar{x}$ and $\bar{y}$ are normalized surface coordinates.

For a Chebyshev Polynomial surface, the accuracy of the surface shape depends on the amount of the Chebyshev terms, the higher orders of the Chebyshev polynomials express the richer details on the surface. In our optimization, the maximum orders in x and y dimensions we used are up to 14. After establishing initial parameters for the ordinary microlens arrays as

Optics EXPRESS

the starting form in the first step, the remaining work is to figure out the optimal coefficients for the polynomials by mathematical method. In the optimization, an orthogonal descent algorithm [34] was used to reduce the standard deviation (rms) of the beam profile iteratively. Figure 5 shows the simulated beam shaping and homogenizing results for a couple of axisymmetric beamlets, before optimization and after optimization. Figure 6 shows the freeform surface sag map of the two axisymmetric microlenses after optimaization.

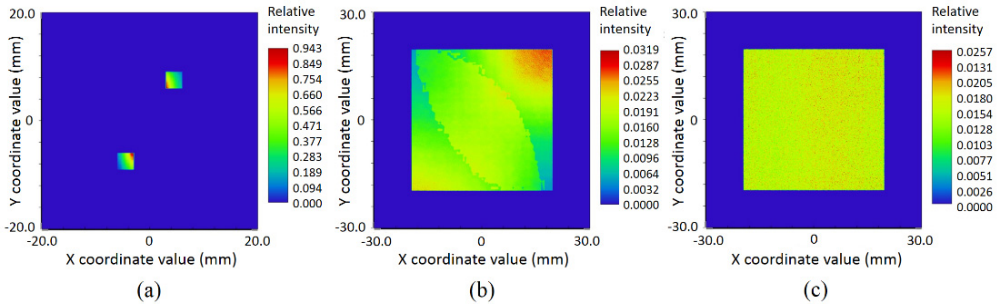

Fig. 5. Simulated beam shaping and homogenizing results for a couple of axisymmetric beamlets. (a) Original intensity distribution of the beamlets, (b) intensity distribution before optimization, and (c) intensity distribution after optimization.

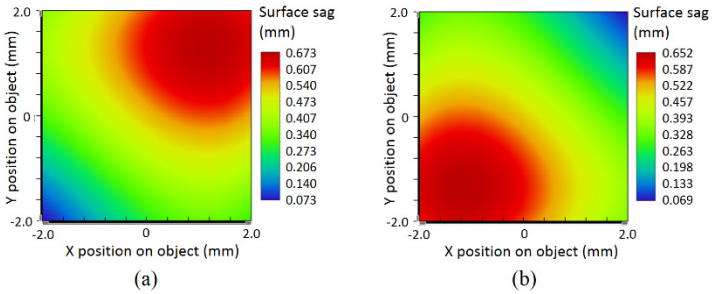

Fig. 6. Surface sag map of the two axisymmetric microlenses after optimization. (a) The upper one and (b) the lower one.

The aperture of the microlens unit is 4 × 4 mm^2, and correspondingly create a 40 × 40 mm^2 square beam pattern at F = 200 mm from the homogenizer, which is a relatively nearby working distance. Comparing the results shown in Figs. 5(b) and 5(c), the deficient energy has been filled up, meanwhile the excess energy has been neutralized in the illumination area. The irradiation becomes obviously uniform after optimization. By the freeform surfaces, wave front aberrations are introduced, and the irradiances of the beamlets are redistributed significantly during propagation.

By repeating this optimization method to each couple of beamlets in the beam from part to whole, the uniformity of the integral beam profile can be improved dramatically. Figure 7 shows the simulated intensity distributions of the final beam shaping and homogenizing results before and after the optimization with freeform microlens arrays.

The amount of the effective freeform microlenses is only 4 × 8 (horizontal vs. vertical), whereas the uniformity of the beam profile can reach within ± 1.3% (rms). It is an excellent level and well qualified for most excimer laser applications. Moreover, the highly uniform beam profile has a large scale and is realized at a relative nearby working distance.

As the phase shift and divergence introduced by the freeform microlenses cannot be compensated by the spherical microlenses in the second array, the output light rays will be distributed irregularly in angular space. Nonetheless, for most imaging exposure processing of excimer lasers, the illuminated mask requires only the uniformity in position space

Optics EXPRESS

(corresponding to the received irradiance in flux per area), and then is further imaged on the wafer by extra imaging optics [12]. For an ideal imaging optical system, wavefront emanating from a single point at the object will be restored to a point at the image. Therefore the ablated pattern is only related to the energy distribution on the mask of the position space, irrespective of the ray irregularity of angular space. More detailed discussion and explanation could be found in [12].

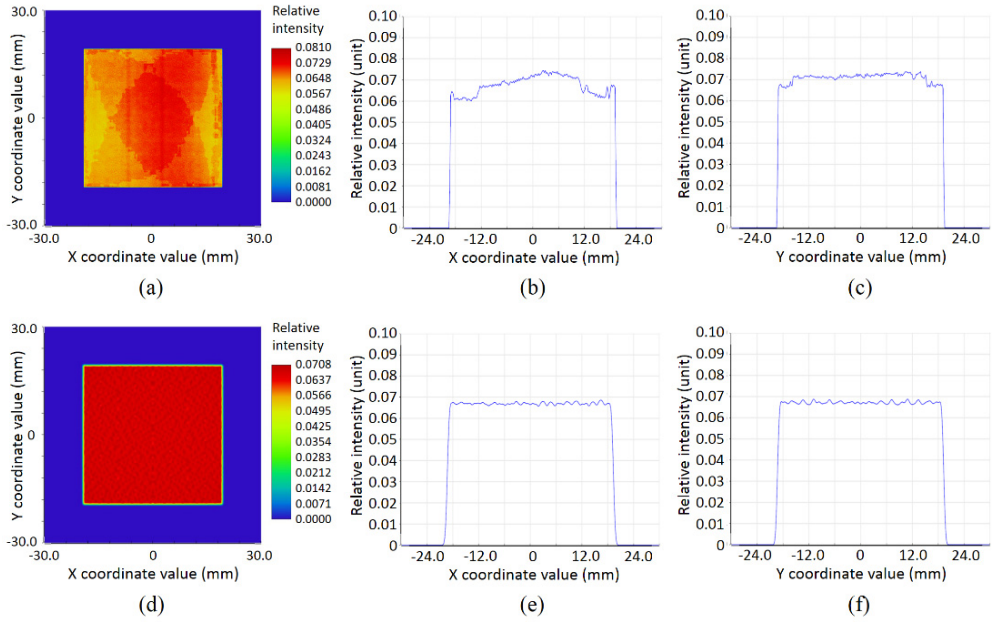

Fig. 7. Comparison of the final beam shaping and homogenizing results before and after optimization. The upper row (a), (b) and (c) show the results by the originally spherical microlens array, including (a) pseudo color intensity distribution, (b) intensity distribution curve in the x direction, and (c) intensity distribution curve in the y direction. The lower row (d), (e) and (f) show the results by the freeform microlens array, including (d) pseudo color intensity distribution, (e) intensity distribution curve in the x direction, and (f) intensity distribution curve in the y direction. After optimization with the freeform microlens array, the uniformity of the beam profile is improved from ± 9.4% (rms) to ± 1.3% (rms), with dimensions of 40 × 40 mm^2.

For the designed homogenizer, the axial position (distance from laser) is not a significant factor to affect the beam shaping result. Because in limited working distance, the divergence of the excimer laser beam does not make significant change on the original beam profile. Whereas slightly lateral adjustment brings only spatial shift of the shaped beam profile. As the working mechanism of the homogenizer is based on the complementation of axisymmetric beamlets, slightly lateral adjustment will not break the tendency. For the beam shaping result, the most significant effect comes from the tilt of the freeform microlens array in space. Because of the employing of freeform surface, each beamlet is introduced specific wavefront aberration, and the distribution status of the light rays on the second microlens surface will be varied. Tilt of the freeform microlens array will lead to some light rays in original beam channel overflow to the neighbor microlens surfaces, thus result in unwanted multiple-images in the homogenization plane. Figure 8 shows the distortions of the homogenized beam profile, when tilting the freeform microlens array 3° about the x, y, and z axes, respectively. The distortions are rendered as energy diffusion and fluctuation for the edges of the beam profile. Comparing between the tilting ways, tilting the freeform microlens array about the z axis makes the most dramatic distortion, as its created light rays overflow is the most direct. The distortion brought by tilt about the y axis is weaker than about the x axis.

Optics EXPRESS

It's related to the asymmetric structure of the effective microlens array in horizontal and vertical directions.

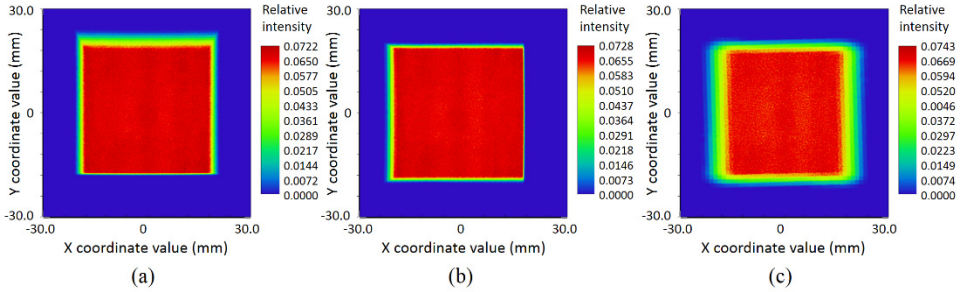

Fig. 8. Beam shaping and homogenizing results when tilting the freeform microlens array. (a), (b) and (c) are the situations when tilting 3° about the x, y and z axes respectively, corresponding to uniformity of ± 3.1% (rms), ± 1.9% (rms) and ± 5.4% (rms) respectively.

4. Experimental testing of the theoretical designed freeform microlens array homogenizer

In order to test the effectiveness of the optical design, we have fabricated the freeform microlens array homogenizer. High purity grade fused silica has been used as the optical material because of its low absorption and degradation at 193 nm wavelength. Each freeform microlens is fabricated individually and then constitutes the microlens array by splicing. A procedural Computer Numerically Controlled (CNC) freeform optics manufacturing technology was used to fabricate the designed freeform surfaces. Detailed process includes surface generation, fine polishing, sub-aperture figure correction, surface smoothing and testing of freeform surfaces. To realize high accuracy and resolution, the metrology of freeform surfaces is achieved by interferometry with Computer Generated Holograms (CGH) for high resolution irregularity measurements. The surface slope tolerance is less than 0.2' (sampling length 1 mm) and the surface roughness is within 10 (Å RMS). Multilayer Anti-reflective (AR) coatings are employed to ensure the transfer efficiency of laser energy. The reflectivity is reduced to less than 0.5% on per surface at 193 nm wavelength (angle of incidence 0°).

To keep the optical components aligning well to each other, all the components are assembled into a high-precision cage system setup which was designed by ourselves, as shown in Fig. 9. The throughout fixed axes are used to ensure the optical axes of the components could be in straight line. For minimizing the departure of the entire optical system from the excimer laser axis, we used a He-Ne laser to calibrate the accurate position for the homogenizer working. Since He-Ne laser has visibility and good collimation, we tested and gave a fine adjustment to make both axes of the He-Ne laser and excimer laser could be overlapped in propagation space, thus the He-Ne laser could be regarded as a reference for alignment. We used the He-Ne laser to calibrate the spatial point positions of the laser input and output for the homogenizer and let the laser throughout the geometric centers of the homogenizer, so that the homogenizer can work in the exact optical axis as designed.

First, to get an intuitional feel for the beam shaping result, we used light-sensitive paper to suffer the irradiation at the target plane. After several consecutive pulses with a stabilized energy of 500 mJ, a clear ablation pattern was leaved on the light-sensitive paper, as shown in Fig. 10(a). The shape of the mark is a standard square, with dimensions of 40 × 40 mm^2. This is consistent with the simulation result. Second, to give a quantitative analysis, we also used the laser beam analyzer to collect the spatial intensity distribution data for the shaped excimer beam profile. The results are shown in Figs. 9(d)-10(b). The initial excimer beam profile has been transformed into an excellent flat-top profile by the homogenizer. The beam uniformity can be stabilized within ± 1.5% (rms) at the working distance of 200 mm. This result is a little

Optics EXPRESS

weaker compared with the simulation. It is mainly caused by the assembling errors, mechanical errors, and the actual performance errors of the optical components.

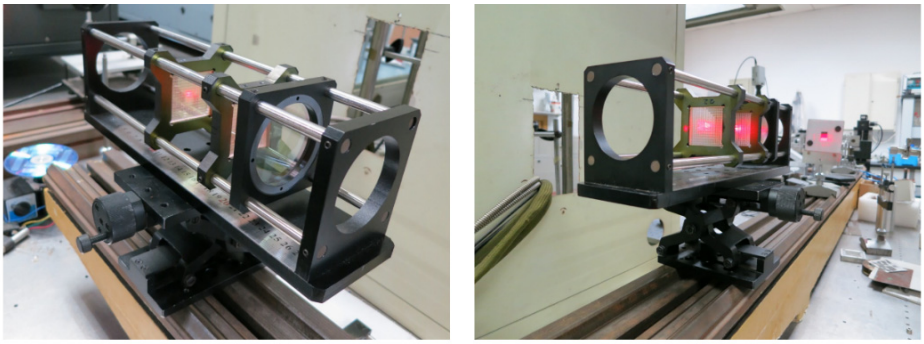

(a) (b)

Fig. 9. The optical cage system setup of the freeform microlens array homogenizer. (a) Front side and (b) back side.

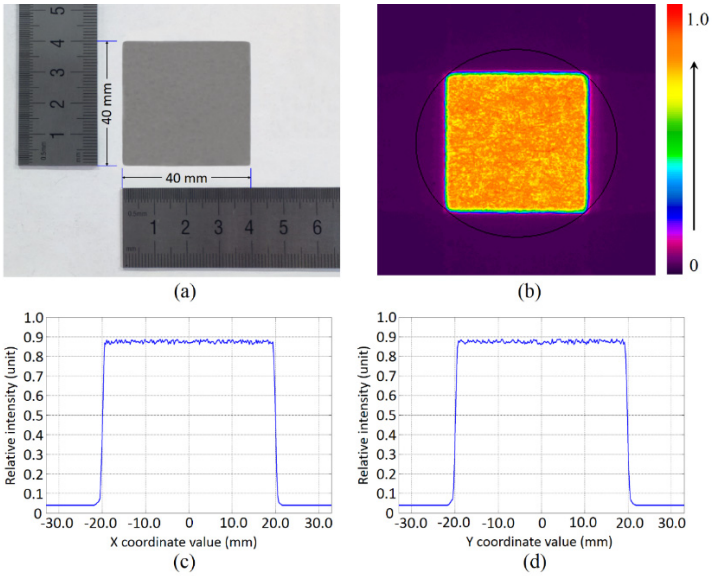

Fig. 10. Experimental results of the freeform microlens array homogenizer. (a) The ablation pattern on light-sensitive paper, (b) pseudo color image of the intensity distribution of the homogenized beam profile, (c) intensity distribution curve in the x direction, and (d) intensity distribution curve in the y direction.

Comparing the result created by conventional microlens arrays, as shown in [19] (microlens unit cell with aperture of 300 × 300μm^2 is used, and a 7.5 × 7.5 mm^2 square flat-top beam profile with uniformity of better than ± 5% (rms) is realized at the work distance of 175 mm), our advance is obvious. Actually, to achieve a good uniformity as our freeform design by conventional one, the aperture of the microlens unit cell should be decreased to micron scale, and correspondingly increasing the amount of the microlenses in thousands, which raises difficulties for fabrication. And to acquire an equivalent illumination with the same size as the freeform one creates, the working distance should be extended by many times. It's not beneficial to the compactness for the system integration. If not so, the large scale illumination at the relative nearby distance has to rely on other magnifying optics. However, the diffraction effect caused by the small aperture of the microlens unit cell will also be magnified, and that can lead to significant diffusion and fluctuation for the energy of

Optics EXPRESS

the beam profile edge. Besides these, the tiny apertures enhance the consequence of misalignment which is unavoidable during practical applications, and that can also give negative effect for the result. Whereas our design can effectively avoid these problems, thus can provide better beam shaping results.

It is worth noting that, the designed homogenizer belongs to static optical system, and the homogenizing result is associated with the original input laser beam profile. The energy level of laser pulse could hardly affect the beam shaping result because the homogenizing mechanism is only based on the relative intensity distribution of the input beam profile. However, for most excimer lasers, the beam profiles could be distorted by unforeseen working condition changes, like resonator readjustment, driving voltage fluctuation, gas deterioration, or window contamination, etc. If the distortion or variation of the input beam profile goes beyond the tolerance of the homogenizer, the homogenizing result will be negatively affected. In the situations, further optical design is needed. In addition, our design method works for a specific individual excimer laser. The specific homogenizer is not universal for other excimer lasers with significantly different beam profiles or different wavelengths. New design is needed if using our method on different lasers.

5. Conclusion

We have presented a novel method to design microlens beam homogenizing optical system for excimer laser. As a new approach we applied a freeform surface microlens array as the first optical component of the homogenizer. Each effective freeform surface in the array can introduce appropriate aberrations in the wave front to redistribute the irradiance of the splitting beamlet. After beam shaping, large scale and highly uniform beam profile was realized at a relative nearby working distance. This is hard to achieve by conventional methods. The design method has been demonstrated as a design instance for a 193 nm excimer laser in our laboratory. The designed homogenizer has been tested, and the experimental results coincide well with the simulations.

Funding

National Natural Science Foundation of China (NSFC) (11374031); Major B Program of Beijing Natural Science Foundation (JC101311201201).

Acknowledgments

Thanks to Zemax, LLC for providing the license of Optic Studio.